



Synthesis, structures and electronic properties of Co(III) complexes with 2-quinolinecarboxaldehyde thio- and selenosemicarbazone: A combined experimental and theoretical study

IVANA S. DJORDJEVIĆ^{1**}, JELENA VUKAŠINOVIĆ², TAMARA R. TODOROVIĆ^{3#},
NENAD R. FILIPOVIĆ^{4#}, MARKO V. RODIĆ⁵, ALEKSANDAR LOLIĆ³,
GUSTAVO PORTALONE⁶, MARIO ZLATOVIĆ^{3#} and SONJA GRUBIŠIĆ^{1*}

¹Institute of Chemistry, Technology and Metallurgy, University of Belgrade, Njegoševa 12, 11001 Belgrade, Serbia, ²Institute for Multidisciplinary Research, University of Belgrade, Volgina 15, 11060 Belgrade, Serbia, ³Faculty of Chemistry, University of Belgrade, Studentski trg 12–16, 11001 Belgrade, Serbia, ⁴Faculty of Agriculture, University of Belgrade, Nemanjina 6, Zemun, Serbia, ⁵Department of Chemistry, Faculty of Sciences, University of Novi Sad, Trg Dositeja Obradovića 4, Novi Sad, Serbia and ⁶Department of Chemistry, Sapienza University of Rome, P.le Aldo Moro 5, 00185 Rome, Italy

(Received 4 April, revised 28 April, accepted 4 May 2017)

Abstract: Cobalt(III) complexes derived from thio- and selenosemicarbazone ligands have been studied to elucidate the nature and consequences of S to Se substitution on their possible biological activity. Solid state structures of cobalt(III) complexes with bis-tridentate coordinated 2-quinolinecarboxaldehyde thio- and selenosemicarbazone were determined by single crystal X-ray diffraction analysis. The complexes were also characterized by spectroscopic methods and cyclic voltammetry. Electronic properties of the complexes were studied using DFT and TD-DFT methods. Finally, evident *in vitro* antioxidant activity of the complexes was demonstrated.

Keywords: X-ray crystal structure; cobalt(III); Schiff base; antioxidant activity; DFT; Fukui.

INTRODUCTION

Schiff bases are some of the most commonly used organic compounds not only with a variety of industrial applications, as pigments and dyes,^{1,2} lasers and non-linear optical systems,^{3,4} optical data storage⁵ and dye-sensitized solar cells,^{6,7} but also with very diverse pharmacological applications.⁸ Derivatives of

*** Corresponding authors. E-mail: (*)grubisic@chem.bg.ac.rs;

(**)ivana.djordjevic@chem.bg.ac.rs

Serbian Chemical Society member.

<https://doi.org/10.2298/JSC170412062D>

Schiff bases, the hydrazone- and semicarbazone-type ligands, have attracted the interest of researchers owing to their diverse chelating properties as ligands containing different NNN, NNO or NNS donor sites.^{9–11} In addition, they coordinate both in neutral and anionic forms generating mononuclear or binuclear metal complexes.^{12,13}

Thiosemicarbazones and their transition metal complexes were extensively studied as potential bioactive compounds showing a broad range of biological properties, such as antifungal, antibacterial, anticancer and cytotoxic activity.^{14–18} On the other hand, cobalt plays crucial roles in many important biological functions and bonding ability towards active sites of enzymes.¹⁹ Cobalt complexes with thiosemicarbazones showed more pronounced biological activity compared to the free ligands.¹⁵ Thione (C=S) and selenone (C=Se) compounds are well known antioxidants that can prevent oxidative damage. Numerous animal and clinical trials investigated the ability of these compounds to prevent oxidative stress that is an underlying cause of cardiovascular disease, Alzheimer's disease, and cancer.²⁰ One comparative study showed that selenosemicarbazones are more potent antioxidants than their sulfur isosteres.²¹

There are fewer studies on selenosemicarbazones and their complexes in comparison to their sulfur and oxygen analogues. It is well known that selenium can substitute the sulfur of the amino acids cysteine and methionine, and that it plays a significant role in biochemical processes as a constituent of selenoproteins. A better understanding of the nature and consequences of this substitution were the main goals of many recent biochemical and theoretical studies.^{22,23}

Herein, the syntheses and crystal structures of Co(III) complexes with thiosemicarbazone and selenosemicarbazone ligands are reported. To obtain detailed characterization of these compounds, which could provide a better insight into the structure–activity relationship, cyclic voltammetry, NMR and UV/Vis spectroscopic analyses and the measurement of antioxidant capacity are presented together with a theoretical study.

EXPERIMENTAL

Materials and methods

Selenosemicarbazide and 2-quinolinecarboxaldehyde were obtained from Acros Organics (BVBA, Geel, Belgium), while thiosemicarbazide and cobalt(II) perchlorate hexahydrate were purchased from Aldrich (Sigma–Aldrich). All solvents (reagent grade) were obtained from commercial suppliers and used without further purification. Infrared (IR) spectra were recorded on a Thermo Scientific Nicolet 6700 FT-IR spectrometer using the attenuated total reflection (ATR) technique in the region 4000–400 cm⁻¹. The NMR spectra were recorded on a Bruker Avance 500 instrument equipped with broad-band direct probe in DMSO-*d*₆. Chemical shifts are given as δ on the ppm scale relative to tetramethylsilane (TMS) as an internal standard for the ¹H- and ¹³C-spectra. Coupling constants (*J*) are valued in Hz. ¹H-NMR spectrum of the sulfur ligands were obtained using a Varian Gemini 2000 instrument at 200 MHz in DMSO-*d*₆. The UV/Vis spectra were recorded on a UV-1800 Shim-

adzu spectrophotometer in the 250–600 nm range using a 1.0 cm path length quartz cell. The molar conductivity measurement was performed at ambient temperature on a Crison MM41 multimeter. The cyclic voltammetry experiments were performed using an electrochemical cell consisting of a three-electrode system: a glassy carbon electrode (3 mm in diameter, CHI 104), a non-aqueous Ag–Ag⁺ reference electrode with a porous Teflon tip (CHI 112) and a Pt wire as the counter electrode. The reference electrode was filled with 10 mM AgNO₃ solution in 0.1 M tetrabutylammonium perchlorate/dimethyl sulfoxide (TBAP/DMSO). All potentials in the paper are given on Ag/Ag⁺ scale. The potential was swept between –2.0 to 1.0 V at a scan rate of 100 mV s⁻¹ in the anodic positive mode. Measurements were performed at room temperature and all solutions were deaerated for 5 min with nitrogen and the working solutions were kept under nitrogen while recording. The voltammograms of studied compounds were recorded in 0.1 M TBAP/DMSO.

The physical and spectral data for the complexes are given in the Supplementary material to this paper.

Synthesis of bis[2-(2-quinolinyl-κN)methylene]hydrazinecarbothioamidato-κN², κS]cobalt(1+) perchlorate monohydrate, [Co(2qatsc)₂]ClO₄·H₂O (1), and bis[2-(2-quinolinyl-κN)-methylene]hydrazinecarbosenoamidato-κN², κS]cobalt(1+) perchlorate monohydrate, [Co(2qasesc)₂]ClO₄·H₂O (2)

2-Quinolinecarboxaldehyde thiosemicarbazone (H2qatsc) and 2-quinolinecarboxaldehyde selenosemicarbazone (H2qasesc) were obtained by condensation of 2-quinolinecarboxaldehyde with thiosemicarbazide/selenosemicarbazide according to reported literature procedures.^{17,24,25} The purity of the synthesized compounds was tested by elemental analysis. IR and NMR spectroscopy data, which were in good agreement with the previously published data.^{17,25} The IR and ¹H-NMR spectra of H2qatsc and H2qasesc are given in Figs. S-3–S-6 of the Supplementary material.

The title complexes were synthesized by a template reaction according to the general procedure: a mixture of 2-quinolinecarboxaldehyde (0.10 g, 0.64 mmol), thiosemicarbazide (0.057 g, 0.63 mmol) or selenosemicarbazide (0.087 g, 0.63 mmol) and Co(ClO₄)₂·6H₂O (0.115 g, 0.315 mmol) in ethanol (15 mL) was refluxed with stirring for 30 min followed by cooling to room temperature. A brown precipitate was filtered off and washed with cold ethanol and diethyl ether. The same products were also obtained by direct synthesis using the starting metal salts and corresponding ligands. Single dark brown crystals were obtained by recrystallization using methanol as the solvent.

NMR spectra of **1** and **2** are given in Figs. S-7–S-10 of the Supplementary material.

X-Ray diffraction analysis (XRD)

The single crystal X-ray diffraction data were collected on a Gemini S diffractometer (Oxford Diffraction) equipped with a Sapphire CCD detector. Graphite monochromated Mo K_α radiation (λ = 0.71073 Å) was employed in the experiments. CrysAlisPro²⁶ was used for raw data integration and reduction. Structures were solved using the SHELXT program²⁷ and refined by the SHELXL-2014/7 program.²⁸ SHELXLE²⁹ was used as a graphical user interface for the refinement procedures. All non-hydrogen atoms were refined anisotropically. Hydrogen atoms bonded to carbon atoms were treated by a riding model in geometrically idealized positions, while those bonded to nitrogen atoms were located in difference electron density maps and refined with distance restraints. Isotropic displacement parameters of all hydrogen atoms were approximated as $U_{\text{iso}} = 1.2U_{\text{eq}}$ of their parent atoms. In neither complex could the hydrogen atoms belonging to the lattice water molecule be located in the difference

electron density maps. The structures were validated using PLATON³⁰ and Cambridge Structural Database (CSD, v. 5.38, updates Nov. 2016)³¹ using MERCURY CSD.³²

Free radical scavenging antioxidant assay

The hydrogen donating ability was assayed using a protocol for the determination of radical scavenging activity. Compounds were dissolved in pure DMSO and diluted into ten different concentrations. Commercially available free radical 2,2-diphenyl-1-picrylhydrazyl (DPPH) was dissolved in methanol at a concentration of 6.58×10^{-5} M. Into a 96-well microplate, 140 μ L of DPPH solution was loaded and 10 μ L DMSO solution of the tested compounds was added, or pure DMSO (10 μ L) in the case of the control. The microplate was incubated for 30 min at 298 K in the dark and the absorbance was measured at 517 nm. All the measurements were performed in triplicate. The scavenging activity of the compounds was calculated using the equation:

$$\text{Scavenging activity} = 100(A_{\text{control}} - A_{\text{sample}}) / A_{\text{control}} \quad (1)$$

where A_{sample} and A_{control} refer to the absorbance at 517 nm of DPPH in the sample and control solutions, respectively. The IC_{50} values were calculated from the plotted graph of scavenging activity against the concentrations of the samples. The IC_{50} is defined as the total antioxidant concentration necessary to decrease the amount of the initial DPPH radical by 50%. The IC_{50} values were calculated for all compounds based on the percentage of DPPH radicals scavenged. Ascorbic acid was used as the reference compound (positive control) at concentrations from 50 to 500 μ g mL^{-1} . For the DPPH scavenging activity, the absorbance at 517 nm was measured using a Thermo Scientific Appliskan instrument.

Computational methodology

Density functional theory (DFT) and time-dependent DFT (TD-DFT) calculations were realized using the Gaussian09 program.³³ For the quantum chemical calculations, the typical hybrid B3LYP^{34,35} functional was considered with the polarized 6-311G(d,p) basis set³⁶⁻⁴¹ and cc-pVTZ.⁴² The effect of solvents was included using the polarizable continuum model (PCM).⁴³

All calculations were performed under restricted formalism, using the default convergence criteria and without any symmetry constraints. The ground state geometries of both Co(III) complexes were calculated in the gas phase and in DMSO solvent and were verified by frequency calculations. The population analysis and partial atomic charge for Co(III) complexes at the ground state geometry in DMSO solvent were calculated using the natural bond orbital analysis (NBO)⁴⁴ incorporated in Gaussian09.

RESULTS AND DISCUSSION

(Chalcogen)semicarbazone cobalt complexes **1** and **2** were synthesized by template reactions starting from $\text{Co}(\text{ClO}_4)_2 \cdot 6\text{H}_2\text{O}$, 2-quinolinecarboxaldehyde and the corresponding (chalcogen)semicarbazide (mole ratio 1:2:2, respectively). The same products were also obtained by direct reactions of the metal salts and the ligands in a 1:2 mole ratio. The composition of the products was not affected by a change in the mole ratio of the reacting species. The complexes are soluble in MeOH, EtOH, MeCN, DMF and DMSO at room temperature. Molar conductivity measurements showed that both complexes are 1:1 electrolytes. Previously, Fan *et al.*¹⁷ synthesized cobalt(II) complex with H2qatsc ligand starting from

$\text{CoCl}_2 \cdot 6\text{H}_2\text{O}$ when one H2qatsc ligand was coordinated in the neutral and the other in the monoanionic form. In the case of complex **1**, which is diamagnetic in nature, both ligands were coordinated in anionic form as could be evidenced by the absence of the H–N3 signal in $^1\text{H-NMR}$ (11.76 ppm in H2qatsc) spectrum of the complex. The cobalt(III) complex of the H2qasesc ligand with the general formula $[\text{Co}(\text{2qasesc})_2]\text{BF}_4 \cdot 2\text{H}_2\text{O}$ was previously synthesized starting from $\text{Co}(\text{BF}_4)_2 \cdot 6\text{H}_2\text{O}$ and H2qasesc ligand.⁴⁵ Although this complex and **2** shared the same complex cation, due to the different number of crystalline water molecules and different counter-ions, they did not possess the same packing arrangement (*vide infra*).

Description of crystal structures

The crystals of the complexes **1** and **2** are isostructural. The XRD analysis showed that in both cases, the cobalt(III) ion coordinates two deprotonated respective ligands, giving octahedral bischelate cations: $[\text{Co}(\text{2qatsc})_2]^+$ in **1** and $[\text{Co}(\text{2qasesc})_2]^+$ in **2**, both with *mer* geometry. In the outer sphere of the complexes, there is one perchlorate ion and one lattice water molecule. Although the cationic species in **1** and **2** possess a chiral octahedral arrangement, both complexes are racemic compounds since they crystallize in the centric *P*-1 space group. The crystal data and structure determination results are summarized in Table S-I of the Supplementary material. A perspective view of the complex cation in **1** is shown in Fig. 1a, while the most relevant bonding parameters are reported in Table I.

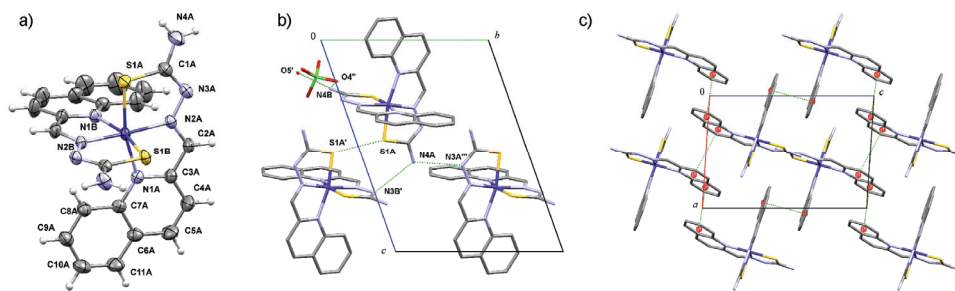


Fig. 1. a) Perspective view and labeling of the molecular structure of $[\text{Co}(\text{2qatsc})_2]^+$ in **1**. Thermal ellipsoids are at the 50 % probability level. b) Crystal packing in the crystal structure of complex **1** viewed along the *a*-axis: hydrogen bonds and van der Waals interaction. c) Crystal packing in the crystal structure of complex **1** viewed along the *b*-axis: π - π stacking interactions of quinoline fragments (green dashed lines); for clarity, perchlorate anions, water solvent molecules and hydrogen atoms are omitted.

The deprotonated ligands coordinate the metal in a tridentate fashion by means of the sulfur (in **1**) or selenium atom (in **2**), the quinoline and the imine nitrogen atoms, forming two five-membered chelate rings. In both complexes the ligand skeletons are essentially planar. However, the chalcogen donor atoms deviate slightly from the average planes formed by the ligands' skeleton (0.11 and 0.18 Å, respectively, for S1A and S1B in **1**, and 0.06 and 0.48 Å, respectively, for Se1A and Se1B in **2**) due to intramolecular repulsion. As previously noticed for the related N4 unsubstituted quinoline-based chalcogensemicarbazone complexes,^{17,45–49} in the crystal structure of **1** and **2**, the chalcogen donors are forced by the bischelate coordination of the ligands to come closer than the sum of their van der Waals radii (**1**: S1A⋯S1B = 3.1914(8) Å, $r_S = 1.80$ Å; **2**: Se1A⋯Se1B = 3.3434(5) Å, $r_{Se} = 1.90$ Å). All metal–donor atom bonds in both complexes are similar to the average corresponding bonds found in a search on quinoline thio/selenosemicarbazone–Co systems performed through the CSD.³¹

TABLE I. Selected bond lengths (Å) and angles (°) for complexes **1** and **2**; X = S in **1**; X = Se in **2**

Bond	Bond lengths		Bond	Angles	
	1	2		1	2
Co(1)–N(2B)	1.8989(15)	1.910(2)	N(2B)–Co(1)–N(2A)	170.31(7)	170.51(10)
Co(1)–N(2A)	1.9020(15)	1.916(2)	N(2B)–Co(1)–N(1B)	81.86(7)	81.74(10)
Co(1)–N(1B)	2.0506(16)	2.054(2)	N(2A)–Co(1)–N(1B)	105.05(7)	104.82(10)
Co(1)–N(1A)	2.0638(16)	2.061(2)	N(2B)–Co(1)–N(1A)	105.07(7)	105.13(10)
Co(1)–X(1B)	2.2241(6)	2.3367(5)	N(2A)–Co(1)–N(1A)	81.71(7)	81.73(10)
Co(1)–X(1A)	2.2246(5)	2.3327(5)	N(1B)–Co(1)–N(1A)	92.40(7)	92.22(10)
C(1A)–N(4A)	1.335(3)	1.333(4)	N(2B)–Co(1)–X(1B)	84.46(5)	84.90(8)
C(1B)–N(4B)	1.333(3)	1.329(5)	N(2A)–Co(1)–X(1B)	88.62(5)	88.52(7)
X(1A)–C(1A)	1.7367(19)	1.885(3)	N(1B)–Co(1)–X(1B)	166.30(5)	166.62(7)
X(1B)–C(1B)	1.737(2)	1.887(3)	N(1A)–Co(1)–X(1B)	90.43(5)	90.60(8)
C(1A)–N(3A)	1.322(3)	1.308(4)	N(2B)–Co(1)–X(1A)	88.83(5)	88.10(7)
C(1B)–N(3B)	1.324(3)	1.313(4)	N(2A)–Co(1)–X(1A)	84.59(5)	85.23(8)
N(2A)–N(3A)	1.371(2)	1.370(3)	N(1B)–Co(1)–X(1A)	88.79(5)	88.79(7)
N(2B)–N(3B)	1.363(2)	1.365(3)	N(1A)–Co(1)–X(1A)	166.08(5)	166.74(7)
N(2A)–C(2A)	1.290(3)	1.281(4)	X(1B)–Co(1)–X(1A)	91.68(2)	91.453(19)
N(2B)–C(2B)	1.293(3)	1.287(4)			

In the crystal structures of both complexes 1-D infinite chains parallel to [010] are formed due to the hydrogen bonding between neighboring complex cations. Perchlorate anions and water molecules also participate in the hydrogen bonding (Fig. 1b). The complex cations in **1** and **2** aggregate in the solid state through weak chalcogen–chalcogen intermolecular interactions (S(1A)⋯S(1A)^{*i*}: 3.334; Se(1A)⋯Se(1A)^{*i*}: 3.289 Å; *i* = 1–*x*, –*y*, 1–*z*). Additionally, there are π – π stacking interactions of the quinoline rings that connect complex molecules into layers parallel to the (101) lattice plane (Fig. 1c). The geometrical parameters

describing hydrogen bonding and π - π interactions in **1** and **2** are given in Table S-II of the Supplementary material.

Optimized geometry

The single crystal structures of the complexes **1** and **2** were used as starting geometries for density functional theory calculations. Atomic numbering for the investigated molecules is shown in Fig. S-1 of the Supplementary material. A previous study showed how the structural parameters of similar cobalt(III) complexes varied with the selected functionals and basis sets.⁹ In the present study, the B3LYP functional was tested with two different size basis sets (Table S-III of the Supplementary material). The results confirmed the tendency increasing bond length with increasing size of the basis set. Therefore, the B3LYP/6-311G(d,p) level was chosen for all geometry optimizations in the gas phase and in the solvent models. The average values of the bond lengths and angles, as well as the ground state geometries of $[\text{Co}(\text{2qatsc})_2]^+$ and $[\text{Co}(\text{2qasesc})_2]^+$ cations, can be found in Table S-IV and Fig. S-2 of the Supplementary material. On comparing the experimental and calculated structural data, it was confirmed that B3LYP/6-311G(d,p) is an acceptable theoretical approach for obtaining the geometries for these systems.

UV/Vis absorption spectra

The UV/Vis spectra for complexes **1** and **2** in DMSO solution showed strong ligand absorption bands dominating mostly in the UV region at wavelengths below 400 nm (Fig. 2).

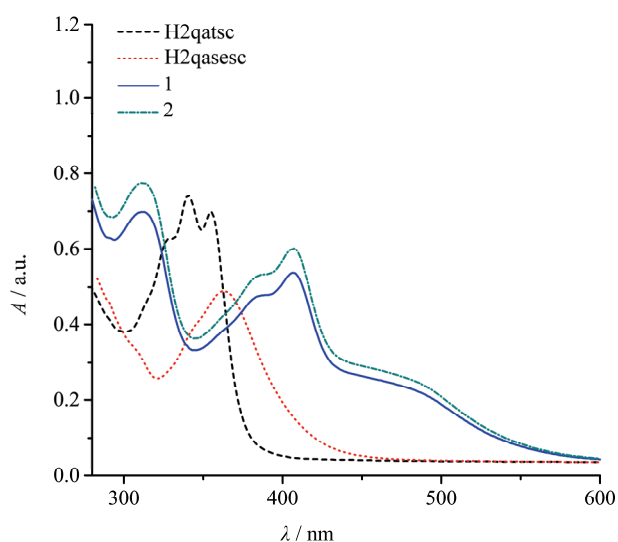


Fig. 2. Experimental UV/Vis spectra of the investigated compounds.

Experimental absorption maxima and TD-DFT/polarizable continuum model (PCM) (DMSO) calculated transitions, together with transition assignments are given in Table II. The first band around 300 nm could be assigned to transition of the quinoline rings.^{9,50} The absorption maxima around 350 nm corresponds to the π - π^* transition of the azomethine group.^{9,51} The presence of intraligand π - π^* transitions, as well as the strong ligand-to-metal charge transfers (LMCT) around 400 nm obscure the weak, spin allowed d-d transitions in the experimental absorption spectra. Based on TD-DFT calculations, the major transitions of the first allowed ${}^1T_{1g} \leftarrow {}^1A_{1g}$ band are at 500 and 570 nm for complexes **1** and **2**, respectively. For the second allowed ${}^1T_{2g} \leftarrow {}^1A_{1g}$ band, the most intense transitions were calculated at 444 and 453, and 466 and 482 nm, for complexes **1** and **2**, respectively. The calculated electronic transitions (λ), oscillator strengths (f) and major MO contributors to the transitions of Co(III) complexes are listed in Tables S-V and S-VI of the Supplementary material. These results are in very good agreement with the previously^{10,52-54} reported UV/Vis absorption maxima of cobalt(III) complexes with similar ligands.

TABLE II. Electronic absorption properties, DFT calculation and assignment of λ (nm) of the investigated compounds in DMSO solvent

Compound	$\lambda_{\text{abs}} / \text{nm}$	The major transitions contributors, nm				
		Assignments				
H2qatsc	329(<i>sh</i>), 340, 355					
H2qasesc	325(<i>sh</i>), 345, 363					
1	311, 389(<i>sh</i>), 406, 441, 493	296, 309	354, 359	390	Assignments	
					${}^1T_{2g} \leftarrow {}^1A_{1g} + \text{LMCT}$	${}^1T_{1g} \leftarrow {}^1A_{1g}$
2	311, 388(<i>sh</i>), 406, 490, 579	306, 309	367, 371	408	Assignments	
					${}^1T_{2g} \leftarrow {}^1A_{1g} + \text{LMCT}$	${}^1T_{1g} \leftarrow {}^1A_{1g}$

Tyler *et al.*⁵⁵ studied the oxidation of thiolato sulfur in model Co(III) complexes for nitrile hydratase, whereby the authors observed that only Co(III) complexes with coordinated thiolato sulfur exhibited absorption around 450 nm, whereas those with coordinated O-bonded sulfonate and S-bonded sulfinate group exhibited a weak band around 520 nm and no absorption at 450 nm. A strong absorption in the 410–450 nm range is also characteristic for Co-containing nitrile hydratase.^{55,56} Since the thiosemicarbazone ligands are not expected to be chromophoric in this range, the significant contribution to these absorptions probably originates from S \rightarrow Co(III) charge transfers.

Graphic representations of the calculated HOMO, LUMO and HOMO–LUMO transitions for the complexes are shown in Fig. 3. The main contribution to the HOMO orbitals of all Co(III) complexes derives from the Se/S atom, metal center and hydrazone group. The higher participation of Se atoms in the HOMO orbital is the main difference between these complexes. The LUMO orbitals of

the complexes are delocalized over all atoms of the ligand (except Se and S) and the metal center.

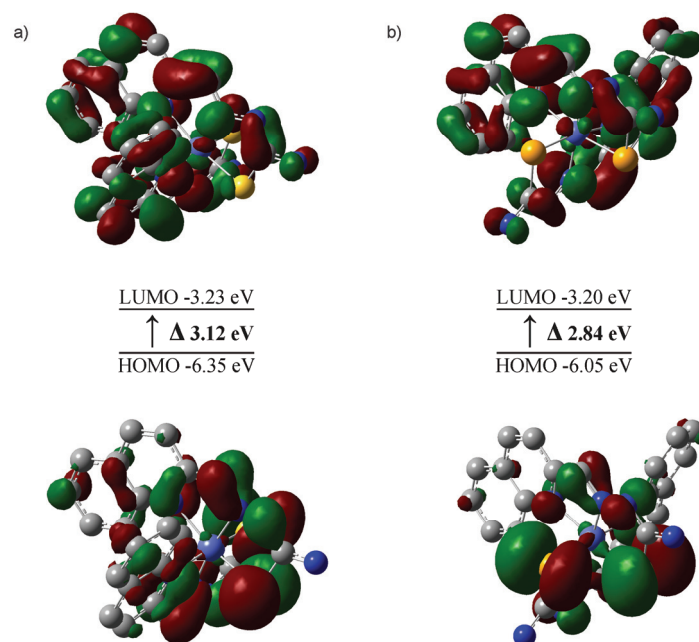


Fig. 3. Graphic representations of the calculated HOMO, LUMO and HOMO–LUMO transitions for: a) complex 1 and b) complex 2.

Cyclic voltammetry

The cyclic voltammogram of Hqatsc (Fig. 4a) shows one reduction peak at -1.72 V and one oxidation peak at 0.68 V. The reduction peak could be attributed to reduction of the thioamide bond.⁵⁷ The cathodic peak for selenoamide reduction is at -1.66 V, and two oxidation peaks at 0.20 and 0.95 V for H2qasesc (Fig. 4b).⁵⁸

The present cobalt complexes showed similar electrochemical behavior to cobalt complexes with different ligands,⁹ *i.e.*, there are two pairs of apparently reversible one-electron peaks (at about -0.70 and -1.50 V). These reversible peaks belong to the reductions $\text{Co(III)} \rightarrow \text{Co(II)}$ and $\text{Co(II)} \rightarrow \text{Co(I)}$. The complex with the H2qasesc ligand showed an additional reduction peak at -1.77 V, which belongs to selenoamide reduction. The peak is about 100 mV more negative compared to that of the free ligand, and the selenoamide bond is still available for reduction, which is hindered due to structural changes. Complex 2 showed an additional oxidation peak at 0.45 V, which could be due to the oxidation of the ligand (0.20 V). Both complexes have additional oxidation peaks at around 0.9 V (Fig. 4).

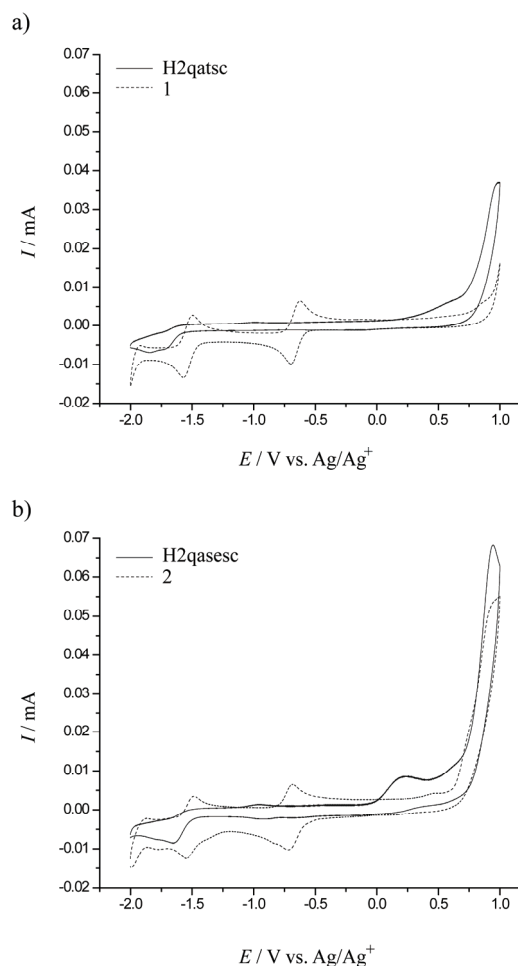


Fig. 4. Representative cyclic voltammograms of: a) H2qatsec free ligand and complex **1** and b) H2qasesc free ligand and complex **2**.

Free-radical scavenging activity

The hydrogen donating ability of investigated compounds was assayed using a protocol for the determination of radical scavenging activity, *i.e.*, the DPPH method.⁵⁸ The radical scavenging activity of the investigated compounds are presented in Table III.

The obtained results revealed that H2qasesc is a better antioxidant than H2qatsec and vitamin C. Complexation of the chalcogensemicarbazone ligands with Co(III) had different impacts on free-radical scavenging activity. Significant reduction of activity was observed for **2** in comparison to free H2qasesc. The same trend was observed in the case of 8-quinolinecarboxaldehyde selenosemicarbazone (H8qsec) and its Co(III) complex⁴⁷ as well in the case of Pd(II), Pt(II) and Zn(II) complexes with quinoline based selenosemicarbazones.^{57,59} In the

case of complexation of H2qatsc with Co(III), an increase in the free-radical scavenging activity was observed. Namely, the activity of **1** almost reached the level of ascorbic acid. A similar trend was also observed in the case of several Co(III) complexes with N-heteroaromatic thiosemicarbazone ligands that coordinate in the NNS tridentate fashion.⁶⁰ The impact of Co(III) coordination on free-radical antioxidant activity is an interesting topic, which will be the subject of more detailed investigations in our group.

TABLE III. IC_{50} values of the DPPH free-radical scavenging activity of the investigated compounds

Compound	IC_{50} / mM (DPPH)
H2qatsc	1.9000
H2qasesc	0.0125
1	0.0883
2	5.1500
Ascorbic acid	0.0793

Fukui functions

Analysis of electron density is fundamental for understanding the chemical reactivity of molecules. One of the most effective tools for the investigation of molecular reactivity was proposed by Parr and Yang,^{61–64} who showed that sites in chemical species with the largest values of Fukui function $f(r)$ are those with higher reactivity. This model relies on the density functional theory and is frequently employed for organic molecules, but rarely used for transition metal complexes. The Fukui $f(r)$ function is defined as the change in electron density upon a change in the number of electrons (Eq. (2)), where $\rho(r)$ is the total electron density of the molecule, N is the number of electrons and $v(r)$ is the external potential exerted by the nucleus. Here, the condensed Fukui function was used to evaluate the reactivity of Co(III) complexes towards nucleophilic, electrophilic and radical attack (Eq. (3)–(5), respectively), where q_N , q_{N+1} and q_{N-1} are partial charges of the atom A in neutral, anionic and cationic forms, respectively. The partial atomic charge for Co(III) complexes was calculated from the natural bond orbital analysis (NBO) at the ground state geometry in DMSO solvent:

$$f(r) = \left(\frac{\partial \rho(r)}{\partial N} \right)_{v(r)} \quad (2)$$

$$f_A^+ = q_N^A - q_{N+1}^A \quad (3)$$

$$f_A^- = q_{N-1}^A - q_N^A \quad (4)$$

$$f_A^0 = \frac{1}{2}(q_{N-1}^A - q_{N+1}^A) \quad (5)$$

According to the results listed in Table IV, the most reactive sites of the molecules upon nucleophilic attack are Se, S and C5 atoms, with very similar values of f^+ . The highest values of f^- are at Se, S, N3 and C2 atoms.

TABLE IV. Values of the Fukui function (a.u.) for Co complexes, considering the NBO charges according with Eqs. (3)–(5)

Compound / atom	f	S/Se	N3	C5	C2
1	f^+	0.056	0.023	0.059	0.039
	f^-	0.135	0.096	0.011	0.070
	f^0	0.095	0.059	0.035	0.054
2	f^+	0.065	0.020	0.058	0.038
	f^-	0.268	0.063	0.014	0.049
	f^0	0.167	0.042	0.036	0.044

Thus, these Co(III) complexes will act as electrophiles in a similar manner during nucleophilic attack. In the case of electrophilic attack, the complexes behavior could be different due to a predominant participation of Se atoms in the HOMO of complex **2** (Fig. 3). Although the LUMO has a similar nature in both complexes, the HOMO has a different composition. In addition, complex **1** has higher values of f^- and f^0 for the N3 and C2 atoms, which could cause different effects during electrophilic and radical attacks.

CONCLUSIONS

Based on known examples of the biological activity of thiosemicarbazone metal complexes, as well as on the proven biological functions of cobalt, the aim of this work was to investigate thio- and selenosemicarbazone complexes of cobalt(III) to elucidate the nature and consequences of S to Se substitution on their possible biological function. Two isostructural complexes, [Co(2qatsc)₂](ClO₄)·H₂O and [Co(2qasesc)₂](ClO₄)·H₂O, were selected and characterized by single crystal XRD analysis, as well as by spectroscopic, and electrochemical methods. Single crystal XRD determined octahedral bis-tridentate meridional coordination of both ligands and a racemic packing mode of individual chiral complexes paired up in the unit cell. An interesting feature of the crystal structure of both complexes is the presence of 1-D infinite chains of hydrogen bonds, as well as strong π - π stacking interactions of neighboring quinoline rings. The geometry optimizations in quantum mechanics (QM) calculations required for analysis of electronic spectra were performed starting from the geometries obtained by XRD. The agreement between calculated and experimental structural data confirmed the reliability of the adopted QM model, and validated the assignment of electronic (UV/Vis) spectra on the basis of TD-DFT calculated transitions. Overall a very good agreement with the previously reported absorption maxima of similar cobalt(III) complexes was achieved. Further insight into the physicochemical properties of the complexes was obtained from cyclic volt-

ammetry, which indicated a possible reduction process of the cobalt atom, as well as redox transformations on the ligands. The DFT calculations provided yet another way to assess the reactivity of the complexes, *i.e.*, through the Fukui functions that indicated the reactive centers most susceptible to nucleophilic, electrophilic, or radical attacks. Finally, the *in vitro* antioxidant activity, assayed by the DPPH method, revealed that the free selenosemicarbazone ligand is a more active scavenger than ascorbic acid as opposed to its cobalt(III) complex, whereas the sulfur isosteres showed an inverse behavior. This peculiar behavior was observed in some other closely related cobalt(III) thiosemicarbazone complexes, but never fully explained. and hence, this will be the subject of further investigations in our group.

SUPPLEMENTARY MATERIAL

Crystallographic data for the complexes have been deposited with the Cambridge Crystallographic Data Centre as Supplementary Publication No. CCDC 1543432-1543433. A copy of these data can be obtained, free of charge, *via* <https://summary.ccdc.cam.ac.uk/structure-summary-form>, or by emailing data_request@ccdc.cam.ac.uk.

X-ray structural and computational data, as well as, the physical and spectral data for the ligands and complexes, together with the ^1H -NMR spectra of all compounds and the ^{13}C -NMR spectra of both complexes are available electronically at the pages of journal website: <http://www.shd.org.rs/JSCS/>, or from the corresponding author on request.

Acknowledgements. The Ministry of Education, Science and Technological Development of the Republic of Serbia supported this work under Grants No. 172035 and 172055.

ИЗВОД

СИНТЕЗА, СТРУКТУРЕ И ЕЛЕКТРОНСКА СВОЈСТВА КОМПЛЕКСА Co(III) СА 2-ХИНОЛИНКАРБАЛДЕХИД-ТИО/СЕЛЕНОСЕМИКАРБАЗОНОМ: ЕКСПЕРИМЕНТАЛНО И ТЕОРИЈСКО ПРОУЧАВАЊЕ

ИВАНА С. БОРЂЕВИЋ¹, ЈЕЛЕНА ВУКАШИНОВИЋ², ТАМАРА Р. ТОДОРОВИЋ³, НЕНАД Р. ФИЛИПОВИЋ⁴,
МАРКО В. РОДИЋ⁵, АЛЕКСАНДАР ЛОЛИЋ³, GUSTAVO PORTALONE⁶, МАРИО ЗЛАТОВИЋ³
и СОЊА ГРУБИШИЋ¹

¹Институт за хемију, технологију и металургију, Универзитет у Београду, Њешићева 12, 11001 Београд, ²Институт за мултидисциплинарна истраживања, Универзитет у Београду, Волгина 15, 11060 Београд, ³Хемијски факултет, Универзитет у Београду, Студентски центар 12–16, 11001 Београд, ⁴Пољопривредни факултет, Универзитет у Београду, Немањина 6, 11080 Земун, ⁵Дејаршман за хемију, Природно-математички факултет, Универзитет у Новом Сагу, Три Досијеја Обрадовића 4, 21000 Нови Сад и ⁶Department of Chemistry, Sapienza University of Rome, P.le Aldo Moro 5, 00185 Rome, Italy

Комплекси кобалта(III) са дериватима тио- и селеносемикарбазона проучавани су како би се разјаснила природа супституције сумпора атомом селена, као и последице ове супституције на њихову потенцијалну биолошку активност. Кристалне структуре комплекса кобалта(III) са бис-тридентатно координованим 2-хинолинкарбалдехид-тио/селеносемикарбазоном одређене су применом дифракције X-зрака на монокристалу. Комплекси су окарактерисани применом спектроскопских метода и цикличном волтаметријом. Електронска својства комплекса испитивана су применом DFT и TD-DFT метода. Такође, потврђена је *in vitro* антиоксидативна активност комплекса.

(Примљено 4. априла, ревидирано 28. априла, прихваћено 4. маја 2017)

REFERENCES

1. X.-C. Chen, T. Tao, Y.-G. Wang, Y.-X. Peng, W. Huang, H.-F. Qian, *Dalton Trans.* **41** (2012) 11107
2. A. D. Towns, *Dyes Pigm.* **42** (1999) 3
3. E. Sternberg, D. Dolphin, *Medical Applications*, in *Infrared Absorbing Dyes*, M. Matsuoka, Ed., Plenum Press, New York, NY, 1990, p. 193
4. A. Abbotto, L. Beverina, N. Manfredi, G. A. Pagani, G. Archetti, H. G. Kuball, C. Wittenburg, J. Heck, J. Holtmann, *Chem. Eur. J.* **15** (2009) 6175
5. S. Kawata, Y. Kawata, *Chem. Rev.* **100** (2000) 1777
6. H. P. Zhou, F. X. Zhou, S. Y. Tang, P. Wu, Y. X. Chen, Y. L. Tu, J. Y. Wu, Y. P. Tian, *Dyes Pigm.* **92** (2012) 633
7. D. E. Mekkawi, M. S. A. Abdel-Mottaleb, *Int. J. Photoenergy* **7** (2005) 95
8. C. M. da Silva, D. L. da Silva, L. V. Modolo, R. B. Alves, M. A. de Resende, C. V. B. Martins, Â. de Fátima, *J. Adv. Res.* **2** (2011) 1
9. N. R. Filipović, H. Elshafly, S. Grubišić, L. S. Jovanović, M. Rodić, I. Novaković, A. Malešević, I. S. Djordjević, H. Li, N. Sojić, A. Marinković, T. R. Todorović, *Dalton Trans.* **46** (2017) 2910
10. B. Shaabani, A. A. Khandar, F. Mahmoudi, S. S. Balula, L. Cunha-Silva, *J. Mol. Struct.* **1045** (2013) 55
11. B. K. Koo, *Bull. Korean Chem. Soc.* **32** (2011) 1729
12. A. Ray, S. Banerjee, R. J. Butcher, C. Desplanches, S. Mitra, *Polyhedron* **27** (2008) 2409
13. A. Bonardi, C. Merlo, C. Pelizzi, G. Pelizzi, P. Tarasconi, F. Vitali, F. Cavatorta, *J. Chem. Soc. Dalton Trans.* **4** (1991) 1063
14. M. Mohan, P. Sharma, *Inorg. Chim. Acta* **106** (1985) 117
15. V. K. Sharma, S. Srivastava, *J. Coord. Chem.* **61** (2008) 178
16. D. Zhang, Q. Li, M.-X. Li, D.-Y. Chen, J.-Y. Niu, *J. Coord. Chem.* **63** (2010) 1063
17. X. Fan, J. Dong, R. Min, Y. Chen, X. Yi, J. Zhou, S. Zhang, *J. Coord. Chem.* **66** (2013) 4268
18. J. García-Tojal, A. García-Orad, A. A. Díaz, J. L. Serra, M. K. Urtiaga, M. I. Arriortua, T. Rojof, *J. Inorg. Biochem.* **84** (2001) 271
19. M. Kobayashi, S. Shimizu, *Eur. J. Biochem.* **261** (1999) 1
20. M. T. Zimmerman, C. A. Bayse, R. R. Ramoutar, J. L. Brumaghim, *J. Inorg. Biochem.* **145** (2015) 30
21. V. Calcaterra, Ó. López, J. G. Fernández-Bolaños, G. B. Plata, J. M. Padrón, *Eur. J. Med. Chem.* **94** (2015) 63
22. S. Schaefer-Ramadan, C. Thorpe, S. Rozovsky, *Arch. Biochem. Biophys.* **548** (2014) 60
23. M. Saberinasab, S. Salehzadeh, Y. Maghsoud, M. Bayat, *Comp. Theor. Chem.* **1078** (2016) 9
24. P. N. Bourosh, M. D. Revenko, M. Gdaniec, E. F. Stratulat, Y. A. Simonov, *J. Struct. Chem.* **50** (2009) 510
25. T. R. Todorović, A. Bacchi, N. O. Juranić, D. M. Sladić, G. Pelizzi, T. Božić, N. R. Filipović, K. K. Anđelković, *Polyhedron* **26** (2007) 3428
26. CrysAlisPro Software system, Rigaku Oxford Diffraction, Oxford, 2015
27. G. M. Sheldrick, *Acta Crystallogr., A* **71** (2015) 3
28. G. M. Sheldrick, *Acta Crystallogr., C* **71** (2015) 3
29. C. B. Hübschle, G. M. Sheldrick, B. Dittrich, *J. Appl. Crystallogr.* **44** (2011) 1281
30. A. L. Spek, *Acta Crystallogr., D* **65** (2009) 148
31. C. R. Groom, I. J. Bruno, M. P. Lightfoot, S. C. Ward, *Acta Crystallogr., B* **72** (2016) 171

32. C. F. Macrae, I. J. Bruno, J. A. Chisholm, P. R. Edgington, P. McCabe, E. Pidcock, L. Rodriguez-Monge, R. Taylor, J. van de Streek, P. A. Wood, *J. Appl. Crystallogr.* **41** (2008) 466
33. *Gaussian 09 (Revision D.01)*, Gaussian, Inc., Wallingford CT, 2009
34. A. D. Becke, *J. Chem. Phys.* **98** (1993) 5648
35. C. Lee, W. Yang, R. G. Parr, *Phys. Rev., B: Condens. Mater. Phys.* **37** (1988) 785
36. A. D. McLean, G. S. Chandler, *J. Chem. Phys.* **72** (1980) 5639
37. K. Raghavachari, J. S. Binkley, R. Seeger, J. A. Pople, *J. Chem. Phys.* **72** (1980) 650
38. A. J. H. Wachters, *J. Chem. Phys.* **52** (1970) 1033
39. P. J. Hay, *J. Chem. Phys.* **66** (1977) 4377
40. K. Raghavachari, G. W. Trucks, *J. Chem. Phys.* **91** (1989) 1062
41. R. C. Binning Jr., L. A. Curtiss, *J. Comput. Chem.* **11** (1990) 1206
42. N. B. Balabanov, K. A. Peterson, *J. Chem. Phys.* **123** (2005) 064107
43. G. Scalmani, M. J. Frisch, *J. Chem. Phys.* **132** (2010) 114110
44. *NBO Version 3.1*, Theoretical Chemistry Institute WISC-TCI, University of Wisconsin-Madison, Madison, 1990
45. T. R. Todorović, A. Bacchi, D. M. Sladić, N. M. Todorović, T. T. Božić, D. D. Radanović, N. R. Filipović, G. Pelizzi, K. K. Anđelković, *Inorg. Chim. Acta* **362** (2009) 3813
46. F. Bisceglie, A. Musiari, S. Pinelli, R. Alinovi, I. Menozzi, E. Polverini, P. Tarasconi, M. Tavone, G. Pelosi, *J. Inorg. Biochem.* **152** (2015) 10
47. N. R. Filipović, S. Bjelogrić, G. Portalone, S. Pelliccia, R. Silvestri, O. Klisurić, M. Senćanski, D. Stanković, T. R. Todorović, C. D. Muller, *MedChemComm* **7** (2016) 1604
48. T. R. Todorović, J. Vukašinović, G. Portalone, S. Suleiman, N. Gligorijević, S. Bjelogrić, K. Jovanović, S. Radulović, K. Anđelković, A. Cassar, N. R. Filipović, P. Schembri-Wismayer, *MedChemComm* **8** (2017) 103
49. P.-D. Mao, L.-L. Yan, W.-J. Wang, Q.-Q. Yang, M.-Q. Cui, Y. Wang, W.-N. Wu, *Wuji Huaxue Xuebao (Chinese J. Inorg. Chem.)*, **32** (2016) 555 (in Chinese with English Abst.)
50. H. N. Ly, D. J. R. Brook, O. Oliverio, *Inorg. Chim. Acta* **378** (2011) 115
51. D. Sek, M. Siwy, K. Bijak, M. Grucela-Zajac, G. Malecki, K. Smolarek, L. Bujak, S. Mackowski, E. Schab-Balcerzak, *J. Phys. Chem. A* **117** (2013) 10320
52. A. Datta, J.-H. Huang, B. Machura, *J. Chem. Crystallogr.* **42** (2012) 691
53. S. K. Chattopadhyay, *Transition Met. Chem.* **22** (1997) 216
54. V. Sunni, M. R. P. Krupp, M. Nathalie, *Polyhedron* **26** (2007) 5203
55. L. A. Tyler, J. C. Overton, M. M. Olmstead, P. K. Mascara, *Inorg. Chem.* **42** (2003) 5751
56. T. Navasota, K. Takeuchi, H. Yamada, *Eur. J. Biochem.* **196** (1991) 581
57. N. R. Filipović, S. Bjelogrić, A. Marinković, T. Ž. Verbić, I. N. Cvijetić, M. Senćanski, M. Rodić, M. Vujčić, D. Sladić, Z. Striković, T. R. Todorović, C. D. Muller, *RSC Adv.* **5** (2015) 95191
58. R. L. Prior, X. Wu, K. Schaech, *J. Agric. Food Chem.* **53** (2005) 4290
59. N. Filipović, N. Polović, B. Rašković, S. Misirlić-Denčić, M. Dulović, M. Savić, M. Nikšić, D. Mitić, K. Anđelković, T. Todorović, *Monatsh. Chem.* **145** (2014) 1089
60. R. Manikandan, P. Viswanathamurthi, K. Velmurugan, R. Nandhakumar, T. Hashimoto, A. Endo, *J. Photochem. Photobiol., B* **130** (2014) 205
61. R. G. Parr, W. Yang, *J. Am. Chem. Soc.* **106** (1984) 4049
62. W. Yang, R. G. Parr, R. Pucci, *J. Chem. Phys.* **81** (1984) 2862
63. W. Yang, R. G. Parr, *Proc. Nat. Acad. Sci. USA* **82** (1985) 6723
64. W. Yang, W. J. Mortier, *J. Am. Chem. Soc.* **108** (1986) 5708.